Biomolecular Damage Induced by Ionizing Radiation: The Direct and Indirect Effects of Low-Energy Electrons on DNA

Elahe Alizadeh,[1] Thomas M. Orlando,[2,3] and Léon Sanche[1]

[1]Groupe en Sciences des Radiations, Département de Médecine Nucléaire et Radiobiologie, Faculté de Médecine et des Sciences de la Santé, Université de Sherbrooke, J1H 5N4 Sherbrooke, Canada

[2]School of Chemistry and Biochemistry and [3]School of Physics, Georgia Institute of Technology, Atlanta, Georgia 30332-0400; email: thomas.orlando@chemistry.gatech.edu

Annu. Rev. Phys. Chem. 2015. 66:379–98

First published online as a Review in Advance on January 12, 2015

The *Annual Review of Physical Chemistry* is online at physchem.annualreviews.org

This article's doi: 10.1146/annurev-physchem-040513-103605

Keywords

dissociative electron attachment, resonance, secondary electrons, strand breaks

Abstract

Many experimental and theoretical advances have recently allowed the study of direct and indirect effects of low-energy electrons (LEEs) on DNA damage. In an effort to explain how LEEs damage the human genome, researchers have focused efforts on LEE interactions with bacterial plasmids, DNA bases, sugar analogs, phosphate groups, and longer DNA moieties. Here, we summarize the current understanding of the fundamental mechanisms involved in LEE-induced damage of DNA and complex biomolecule films. Results obtained by several laboratories on films prepared and analyzed by different methods and irradiated with different electron-beam current densities and fluencies are presented. Despite varied conditions (e.g., film thicknesses and morphologies, intrinsic water content, substrate interactions, and extrinsic atmospheric compositions), comparisons show a striking resemblance in the types of damage produced and their yield functions. The potential of controlling this damage using molecular and nanoparticle targets with high LEE yields in targeted radiation-based cancer therapies is also discussed.

1. INTRODUCTION

High-energy ionizing radiation (e.g., α-, γ-, X-rays, protons, heavy ions) causes a variety of lesions to living cells, which can lead to loss of genetic information, mutation, promotion of genomic instability, and apoptosis (1–3). The most frequent and lethal lesions occurring at the cellular level, which perturb or stop cellular function, are considered to be those affecting the human genome. These include single-strand breaks (SSBs) and double-strand breaks (DSBs), DNA-DNA or DNA-protein cross-links, base release and other chemical modifications, and multiply damaged sites of DNA (4). This damage is induced either by the direct interaction of radiation with any of the individual DNA moieties (5, 6) or by the indirect interaction of the reactive species induced from molecules surrounding DNA (7, 8). The latter, commonly referred to as the indirect effect, concerns the interaction of radiation with the local molecular environment surrounding the DNA molecule (e.g., water, salts, proteins, and oxygen molecules). The indirect effect arises principally from the reaction of water radiolysis products (hydroxyl radicals, solvated electrons, and hydrogen atoms) with DNA. It has been assumed that the damage to the human genome by high-energy radiation is about one-third direct and two-thirds indirect (9). However, this assumption has recently been questioned by ultrafast electron transfer experiments involving DNA (10). These experiments suggest that two-thirds of the damage is direct and one-third is indirect (11).

In both the direct and indirect effects, the energy imparted to the biological media occurs mainly via ionization (12), generating large quantities of secondary species along the radiation track [e.g., ions, radicals, and secondary electrons (SEs)] (13). Nonthermal SEs are the most abundant secondary species, as approximately 5×10^4 are produced per megaelectron volt of deposited energy. Typically, SEs have initial kinetic energies lying below 30 eV and a most probable energy of approximately 9–10 eV (14). These electrons lose energy via inelastic collisions with the molecules of the media, initiating further excitations and ionization processes. Therefore, prior to being thermalized, SEs can induce severe structural and chemical alterations (13).

SEs with energies below 30 eV are referred to as low-energy electrons (LEEs). Remarkably, LEEs damage DNA essentially by attaching temporarily to DNA components, forming transient negative ions (TNIs) of DNA subunits (e.g., a base, sugar, or phosphate group). In this manner, LEEs induce direct damage to DNA, such as SSBs and DSBs via the decay of TNIs into dissociating electronically excited states and dissociative electron attachment (DEA) (15, 16) channels. As a large proportion of cell constituents (almost 70–80%) consist of water, LEEs also interact with water molecules near DNA molecules in the cell nucleus and create reactive species to induce indirect damage (17). Direct LEE-induced DNA damage can be increased by the covalent binding of radiosensitizers and chemotherapeutic agents to the molecule (18, 19). This enhancement was found to be essentially caused by the appearance of new TNIs near the site of binding of the drug or by the preferential enhancement of dissociative channels of pre-existing TNIs, as well as the weakening of chemical bonds within DNA molecules. As recently shown in molecular models and in vitro and animal studies with platinum chemotherapeutic agents and a liposomal formulation of the drugs, a fundamental understanding of the biological action of LEEs with and without chemical modification of DNA can lead to the development of more efficient clinical protocols and radiosensitizing chemotherapeutic agents (20–25).

LEE interactions with various biomolecules and DNA basic constituents in the gas and condensed phase, through the formation of TNIs and resonance states, have been described and summarized in several authoritative review articles (26–30). Thus, in the present review, we discuss (*a*) the basic principles of electron resonances in a large molecule such as DNA, (*b*) the mechanisms involved in LEE-induced damage of dry and wet DNA, (*c*) LEE-induced damage

of DNA interacting with important cellular constituents, and (*d*) the role of LEEs in radiation therapy, including the major mechanisms of LEE-induced damage in living cells.

2. MECHANISMS OF THE DIRECT EFFECTS OF LOW-ENERGY ELECTRONS

Since the discovery that electrons with energies below 15 eV could directly induce SSBs and DSBs in DNA, considerable efforts have been devoted to investigating the precise mechanisms responsible for the damage and its localization on specific bonds (26–28, 31, 32). Relevant experiments have included mass spectrometry investigations (27, 28, 31, 32) and high-resolution electron energy loss (HREEL) spectra measurements (33–36) of the basic molecular components of DNA in their gaseous and condensed phases, as well as chemical analysis of the products resulting from LEE bombardment of multilayer and self-assembled monolayer films of DNA (26–29, 31, 32).

Recently, LEE-induced bond cleavage at the single-molecule level within DNA origami templates was visualized by atomic force microscopy (AFM) (37). This novel technique enables the fast and parallel determination of strand break yields with unprecedented control over the DNA molecule's primary and secondary structure. Another spatially resolved technique exploits the use of graphene-coated gold thin films and surface-enhanced Raman spectroscopy. This technique was recently used to examine the sequence dependence of DNA damage at excitation energies <5 eV (38). Currently, Ptasińska and colleagues (39) are performing a quantitative and qualitative study of the different types of damage to dry and aqueous DNA induced by exposure to helium atmospheric-pressure plasma jets. Because these jets contain multiple types of species found in radiation chemistry, including LEEs, such plasma exposure provides information on the effects of the direct and indirect pathways of damaging DNA. Ptasińska and colleagues (39) applied nitrogen atmospheric-pressure plasma jets to induce DNA damage in SCC-25 oral cancer cells, thus providing insight into radiation damage to a cellular system.

The emission of SEs from a metal surface exposed to soft X-rays is another source of LEEs, which is extensively described in some review articles (26, 40). Recently, angle- and polarization-resolved X-ray photoelectron spectroscopy has also been used to probe DNA damage as a function of the bonding interaction and geometry of DNA adsorbed on gold and thiolated gold substrates (41). Specifically, the angle- and polarization-resolved studies indicated that both the thiolated and unthiolated DNA samples were protruding out and were oriented 45° from the surface normal. Prolonged exposure led to DNA strand breakage, and the damage cross section derived from time-dependent X-ray photoelectron spectroscopic data was found to be significantly higher for the thiolated versus the unthiolated DNA (3.1 ± 0.2 versus 2.5 ± 0.2 Mb). This is likely correlated with the more effective capturing of low-energy SEs in the lowest unoccupied molecular orbital of the thiolated DNA (41). The LEEs emitted from X-ray irradiated metal surfaces can also be exploited to investigate DNA damage under well-defined gaseous atmospheres and specific humidity levels (40).

By comparing the results generated in these various experiments, researchers in many cases have been able to deduce the mechanisms responsible for bond scissions in DNA. Two major types of TNIs located on the basic subunits (31, 33–36) are involved in damage to DNA induced by LEEs: shape resonances, which consist of an electron temporarily occupying a previous unfilled orbital of the ground state of a basic subunit, and core-excited or Feshbach resonances, in which the incoming electron is captured by the positive electron affinity of an electronically excited state (i.e., the parent state) of the subunit (42). When the latter resonance involves an incoming electron with nonzero angular momentum with respect to the capturing site, it is referred to as a core-excited shape resonance. In a small molecule, a TNI can decay by DEA usually with the

concomitant formation of a stable anion and a radical (43). The latter fragments can also be released from DNA, but in such a large biomolecule, chain cleavage, leaving one side with the electron and the other as a radical, is also an important process. Alternatively, autoionization of a core-excited anion site can cause bond rupture by leaving the subunit in a dissociative electronically excited state. This decay channel has been investigated in the condensed phase by measuring the cross sections for electronic excitation of the bases (34–36) and the sugar analogs (44–48) with HREEL spectroscopy and by electron-stimulated desorption (ESD) of neutral fragments from DNA in the 3–20-eV range using mass spectroscopy (49). A similar ESD study has been reported, using frequency tripled lasers and single-photon ionization to detect neutral DNA fragments (50).

Below the energy threshold for electronic excitation (E_e = 3–4 eV), the resonance features in the electron energy dependence of the yields (i.e., the yield functions) of specific damage to DNA or its subunits were interpreted as resulting from the initial formation of shape resonances of the basic subunits, whereas at higher energy, they were interpreted as resulting from the formation of core-excited resonances or core-excited shape resonances. The reasons for these assignments arise from basic considerations and general gas-phase data. In a shape resonance, the additional electron is temporarily retained on a DNA subunit by an angular momentum barrier, which creates, with the other terms of the interaction potential, a quasi-bond state having at least one energy level (51). Scattering electrons are tunneling in and out of the interaction potential with an average residence time defined as the lifetime of the TNI. Shape resonances are therefore strongly coupled to the ground state of the target molecule or basic DNA subunit and thus rarely decay into electronically excited states. Hence, their involvement in fragmentation processes can occur only via DEA to repulsive anion states with ground-state dissociation limits. Moreover, at energies larger than 3–4 eV, the quasi-bound electron in a shape resonance can rapidly tunnel through the interaction potential, so the lifetime of these TNIs is usually not sufficient for DEA to occur. Alternatively, core-excited resonances, which lie above 3–4 eV, have much longer lifetimes and can more easily couple to electronically excited states (52–54). This coupling is particularly effective in the case of a core-excited shape resonance, usually lying 0–1 eV above the energy of its parent electronically excited state, into which it strongly decays. In this case, an electron is captured by both a centripetal potential and the positive electron affinity of an electronically excited state.

At the experimental level, Allan and coworkers (55–59) and others (60–66) observed DEA from core-excited TNI states in the anion yield functions of at least 35 hydrocarbons, including large alcohols, esters, and saturated compounds containing ether and hydroxyl groups. Using the energies of the potential grandparent cation state (i.e., the positive ion core) as a guide, Allan and coworkers (57–59) could assign the peaks in their 5–12-eV anion yield functions to the initial formation of core-excited resonances. Comparison with photoelectron spectra allowed them to establish the nature of the resonance process and the binding energy of the two electrons in Rydberg orbitals around the positive core (55). The σ-type core-excited resonances lying in the 8–11-eV region of large hydrocarbons, which decayed via DEA, did not depend on the nature of the molecule. Their result corroborated with the previous hypothesis that LEEs in even larger molecules such as DNA can also localize around specific bonds or subunits to form core-excited resonances (56).

Several theoretical advances during the past decade have also made it possible to arrive at a fairly good understanding of processes corresponding to the addition of a single electron to a ground-state site of a subunit or small segment of a DNA molecule (30, 44, 67, 68). Owing to the simplicity of such an initial event, as well as the availability of substantial computational resources, the interaction of subexcitation ($E < 3$ eV) electrons could be effectively treated using different calculation methods. Theoretical predictions then provided a fairly detailed understanding of electron capture at specific sites of DNA and the subsequent electron transfer and DEA processes.

Based on both experiments (69) and theoretical studies (30, 44, 67, 68), we know that electrons with energies below 3 eV cleave the C–O bond of the DNA backbone at the 3′ and 5′ positions, to a small extent by direct capture at a phosphate group (70, 71) but primarily via electron transfer from a base to the phosphate group (72–75). In brief, an incoming electron captured by one of the lowest π^* resonance states of the bases (76) transfers to the antibonding σ^* orbital of the C–O bond in the backbone of DNA, where it resides for a sufficiently long time to cause rupture of the σ^* bond. This latter process may also be induced by proton transfer to a negatively charged base during the lifetime of a resonance (77). Such a transfer leaves an extra electron on the sugar or phosphate unit, which can also lead to rupture of the sugar-phosphate C–O bond, again via DEA.

Martin et al. (69) were the first to provide experimental support for the hypothesis of electron transfer from a base to the phosphate group. They measured the 0–4-eV yield function of SSBs in plasmid DNA. They showed the presence of two resonances at 0.8 eV and 2.2 eV by TNI formation, which could be attributed to electron capture by the bases followed by electron transfer to the phosphate group. Later, Zheng et al. (78) bombarded, with 4- to 10-eV electrons, thin molecular films of short single-stranded DNA containing the four bases (i.e., the oligonucleotide GCAT, where G stands for guanine, C for cytosine, A for adenine, and T for thymine) with and without an abasic site (i.e., a location in a DNA strand with a missing purine or pyrimidine) (78). At 6 eV and 10 eV, cleavage of the C–O bond linked to the abasic site was considerably reduced. These results indicated not only that the inhibition of electron transfer from a specific base reduces strand breaks, but also that the electron transfer process found below 3 eV may also be operative up to 10 eV.

Above the energy of the electronic excitation threshold of the basic constituents of DNA (i.e., above 3 eV), the exact mechanisms leading to bond rupture are more difficult to determine; this is largely a result of the formation of core-excited resonances. Calculations on the formation of core-excited TNIs and their decay into harmful products are presently quite limited because of the complexity of theoretically describing multiple electronically excited orbitals. So far, only calculations involving a single electron in a ground or excited molecular orbital have been performed to describe electron scattering or capture by a small DNA strand (30, 44, 67, 68). According to multiple scattering theory (79, 80), the coherent enhancement of the electron wave initially scattered within DNA is relatively small at 9–10 eV, but below 4 eV, it can reach one order of magnitude for $\ell = 2$ partial waves and two orders of magnitude for $\ell = 3$. In general, as the electron energy decreases, the electron wave function becomes larger and more delocalized, and hence diffraction, which is structure dependent, becomes prominent. This phenomenon further illustrates that electron transfer is expected to be favored at low energies; however, it does not provide a mechanism for strand breaks above the energy of electronic excitation.

Conversely, at the experimental level, detailed analyses of the products induced by 4–15-eV and 10-eV electron impact on thin films comprising small oligonucleotides of different lengths indicate that at higher energies, strand breaks also occur predominantly by electron transfer. So far, four different experiments with oligonucleotides have shown that 10-eV electron capture by an inner base in an oligonucleotide leads to electron transfer to the phosphate group (78, 81, 82). To reconcile these results with those of the theoretical and experimental studies below 3 eV, Zheng et al. (78) proposed a two-step process in which, after electronically exciting a base, the incoming electron has much lower energy and hence favorably transfers to the phosphate group, where it ruptures the C–O bond via DEA. This hypothesis has two consequences: (*a*) If an abasic site is created within a DNA strand, the resonances in the yield functions of SSBs, which would normally arise from electron transfer from that site, should disappear, and (*b*) if the electronically excited state is dissociative, a single electron could damage a base and break a strand within an oligonucleotide. Both phenomena have been observed experimentally, the former by Zheng et al.

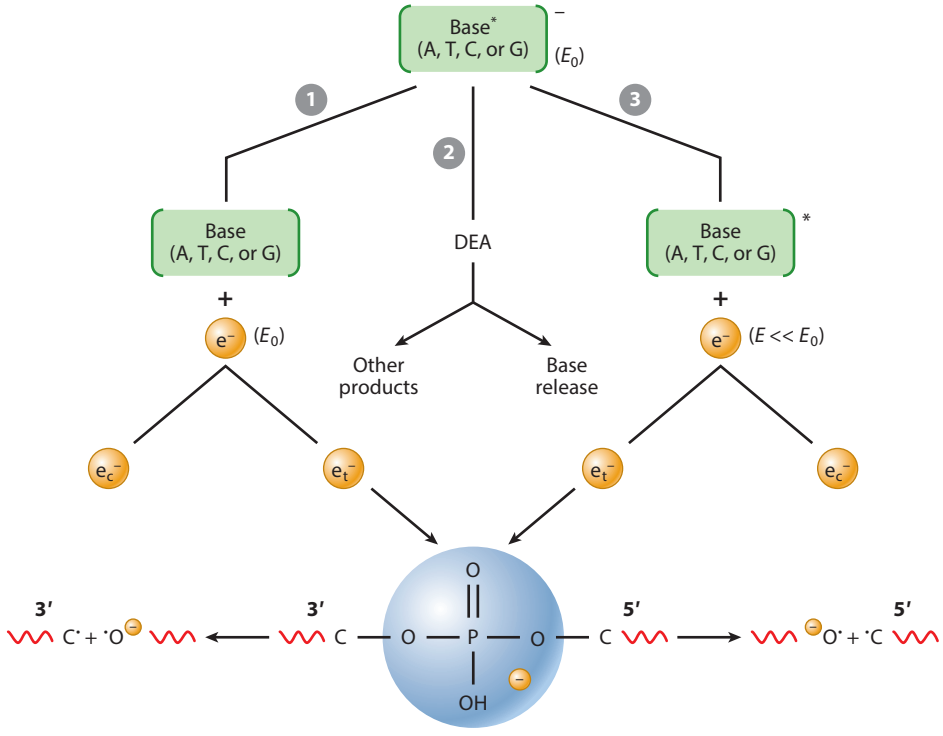

Figure 1

Decay channels of transient negative ions of DNA bases formed at an initial electron energy of E_0. Within DNA, the electron is usually captured by a nucleobase, forming a shape or core-excited resonance. The transient anion can decay into three pathways, which represent ❶ the elastic ($E = E_0$) channel; ❷ the direct dissociative electron attachment (DEA) channel, leading to fragmentation of the parent nucleobase or base release; and ❸ the electronically inelastic ($E \ll E_0$) channel. In pathways ❶ and ❸ the electron can be re-emitted into the continuum (e_c^-) or transfer (e_t^-) within DNA. The extra electron has been found to be capable of transferring to and localizing on the sugar-phosphate group, where it breaks the C–O σ bond via DEA. Breakage of the C–O bond within DNA occurs principally via pathway ❸ for $E_0 > 5$ eV. If the electronically excited state formed via pathway ❸ is dissociative, a single low-energy electron can break two bonds.

(71) in GCAT and the latter by Li et al. (83) in LEE-induced damage to a thymine trinucleotide with the central base substituted with 5-bromouracil.

Taking into consideration the amount of experimental and theoretical evidence, researchers proposed the main routes leading to strand breaks, base release, and base damage in DNA (28) (**Figure 1**). An incoming electron of energy E_0 is preferentially captured via a shape resonance, a core-excited resonance, or a core-excited shape resonance of a base within DNA. When E_0 is lower than approximately 0.5 eV below the energy of the first electronic excitation threshold, only shape resonances can be formed on a base. DEA to a base is possible, and route 1 in **Figure 1** is accessible for electron transfer to the phosphate group or simply autoionization into the elastic continuum. As explained above, via pathway 1, the C–O bond of the DNA backbone is cleaved at the 3′ and 5′ positions. Above the electronic excitation threshold, core-excited types of resonances are expected to lead to dissociation via route 2. Route 3 is the inelastic channel; via this channel, electronic excitation of a base can release a very low energy electron (e.g., $E_0 \simeq -0.5$–1 eV). Only

core-excited resonances and core-excited shape resonances can decay into the inelastic channel. As with route 1, the electron can be re-emitted into the continuum or transfer within DNA to the C–O σ^* bond. The electron transfer probability has been calculated to be large at very low energies (<1 eV) (73–75), and in core-excited resonances or core-excited shape resonances, the additional electron has an energy slightly below (~0.5 eV) or slightly above (~0–1 eV) the vacuum level (0 eV), respectively. This type of TNI is therefore expected to favor electron transfer leading to SSBs in DNA, sometimes accompanied by base damage.

According to the diagram depicted in **Figure 1**, one should find the core-excited resonances of the DNA bases to be initially responsible for most strand breaks in DNA above ~3 eV. Hence, the energy dependence of the capture cross sections of the bases should be reflected in the yield functions of chain scission. The energies of the core-excited resonances of the bases have been measured in the gas (84–91) and condensed (34–36, 49, 91) phases. The latter account for the polarization energy of the medium on the TNI and should therefore be more appropriate for comparison with data from DNA films.

Table 1 lists the most intense core-excited resonances found in different decay channels for the four DNA bases in condensed films. The TNI energies are given in the second column, and the channels in which they were observed in HREEL and ESD experiments are reported in the third column. In the case of decay by autoionization, leaving the base in an electronically excited state, the resulting transition is given, whereas for the DEA channel, we give the maxima in each specific anion yield function. Stacking of the bases probably slightly modifies the resonance energies in **Table 1**. However, the attractive π-π noncovalent interaction between the aromatic rings of the bases is present in the tetramer GCAT, for which DEA peaks lie within the range of approximately 9–11 eV (92, 93) (**Table 1**). Essentially three groups of core-excited resonances (I, II, and III) are found; they are located in the 5–6-eV, 8.5–11-eV, and 12–16-eV regions, respectively.

Figure 2 compares results obtained by different laboratories on different types of damage induced in vacuum by LEE impact on dry DNA films. Conditions that may differ among experiments include the nature of the DNA films (e.g., the length, configuration, and purity of the DNA; film preparation; thickness; uniformity; and substrate), electron-beam current density and fluence, and method of analysis. Despite such varied conditions, there is a striking resemblance in the yield functions shown in **Figure 2*a–e***. **Figure 2*a*** shows the yield function for the loss of the supercoiled configuration of plasmid DNA (pUC21; 3,151 base pairs) uniformly deposited on highly oriented pyrolitic graphite by intercalating doubly charged 1,3-diaminopropane (Dap^{2+}) between each molecule (94). The affinity of Dap^{2+} for DNA permits layer-by-layer growth of plasmid films of uniform thickness that can be measured and monitored by AFM. Owing to the protein-like NH_3^+ group of Dap^{2+}, the binding of Dap^{2+} to DNA in these films is similar to that with proteins in the cell nucleus. The results in **Figure 2*b*** exhibit the yield functions for specific damages to a short DNA strand (i.e., the tetramer GCAT). The curves represent the yield functions for the release of thymine and strand breaks producing pT and pCAT, where p denotes the sugar-phosphate group (95). The products were analyzed by high-performance liquid chromatography (HPLC). The curve in **Figure 2*c*** represents the yield of H^- anions desorbed by electron impact on a film comprising synthetic 25-bp double-stranded DNA and the pGEM 3,199-bp plasmid (96). The curves in **Figure 2*d–g*** represent the yield functions for the production of SSBs from pGEM 3,199-bp plasmid DNA (**Figure 2*d*,*e***) (97), p14 6,360-bp plasmid DNA (**Figure 2*f***) (50, 98), and the pQE30 plasmid DNA (**Figure 2*g***) (99). The curves in **Figure 2*a–f*** clearly show the predominance of a strong maximum lying between 9 and 11 eV. Another peak is visible between 4.5 and 6 eV in the curves in **Figure 2*a*,*b*,*e***. A shoulder is also present in this energy region in the data of Huels et al. (16) (**Figure 2*d***). Another region can be delineated from the curves in **Figure 2*d*,*g***, where a peak appears between 14 and 16 eV.

Table 1 Most intense core-excited resonances formed on the bases and their decay channels below 16 eV

Base/oligonucleotide	Resonance energy (eV)	Decay channels
Thymine (T) (34)	5 (I)	$1^3A'(\pi_2 \rightarrow \pi_3^*) + 1^3A''(n_2 \rightarrow \pi_3^*)$
	8.5 (II)	$2^3A'(\pi_1 \rightarrow \pi_3^*) + 2^1A'(\pi_2 \rightarrow \pi_3^*)$
	8.5 (II)	$3^3A', 2^3A'', 4^3A', 3^3A'', 3^1A'$
	9 (II)	$5^3A'(\pi_0 \rightarrow \pi_3^*) + 5^1A'(\pi_1 \rightarrow \pi_4^*)$
	9.3 (II), 15.9 (III)	DEA (H^-)
	9.9 (II), 13.9 (III)	DEA (CN^-)
	9.8 (II)	DEA (OH^-)
	12.7 (III)	DEA (OCN^-)
	10.7 (II)	DEA (CH_2^-)
Cytosine (C) (35)	6 (I)	$1^3A'(\pi \rightarrow \pi^*)$
	10 (II)	$3^{3,1}A'(\pi \rightarrow \pi^*)$
	11 (II)	$4^1A'(\pi \rightarrow \pi^*)$
	12 (III)	$5^1A'(\pi \rightarrow \pi^*)$
	12 (III)	$6^1A'(\pi \rightarrow \pi^*)$
	8.5 (II), 10.3 (II)	DEA (H^-)
	8.9 (II)	DEA (CN^-)
	8.8 (II)	DEA (O^-)
	11 (II)	Ionization
Adenine (A) (36)	10 (II)	$n \rightarrow \pi^*$
	10 (II)	$\pi \rightarrow \sigma^*$
	10 (II)	$\pi \rightarrow \pi^*$
	9.5 (II), 14.3 (III)	DEA (H^-)
	9.8 (II), 15.3 (III)	DEA (CN^-)
Guanine (G)	10.6 (II), 15.0 (III)	DEA (H^-)
	9.0 (II), 13.9 (III)	DEA (CN^-)
	9.0 (II), 13.2 (III)	DEA (O^-)
	8.7 (II), 12.7 (III)	DEA (OH^-)
GCAT (49)	9.2 (II)	DEA(H^-)
	9.0 (II), 11.3 (II)	DEA (O^-/NH_2^-)
	9.1 (II)	DEA (OH^-)

Dissociative electron attachment (DEA) results were obtained from Reference 49. Table adapted with permission from Reference 97. Copyright 2014, AIP Publishing LLC.

The ranges of the three groups of core-excited resonances (I, II, and III) located in the 5–6-eV, 8.5–11-eV, and 12–16-eV regions in **Table 1** agree well with the energy windows shown in **Figure 2** for the resonances observed in various yield functions by many groups. Three-quarters of the resonance-decay manifold of the bases lie in the 8.5–11-eV region. It is therefore not surprising to find the strongest yields in SSBs located in this energy range. In **Figure 2**, the core-excited resonances lying within the 4–6-eV region correspond to those located at 5 eV and 6 eV in **Table 1** (i.e., group I); these resonances decay by autoionization, leaving the bases thymine or cytosine in the lowest triplet electronically excited states. According to the diagram in **Figure 1**, after creating these states, the autoionizing electron returns to the continuum (e_c) or transfers to the phosphate group (e_t), causing an SSB. From 8.5 to 11 eV, the strong resonance

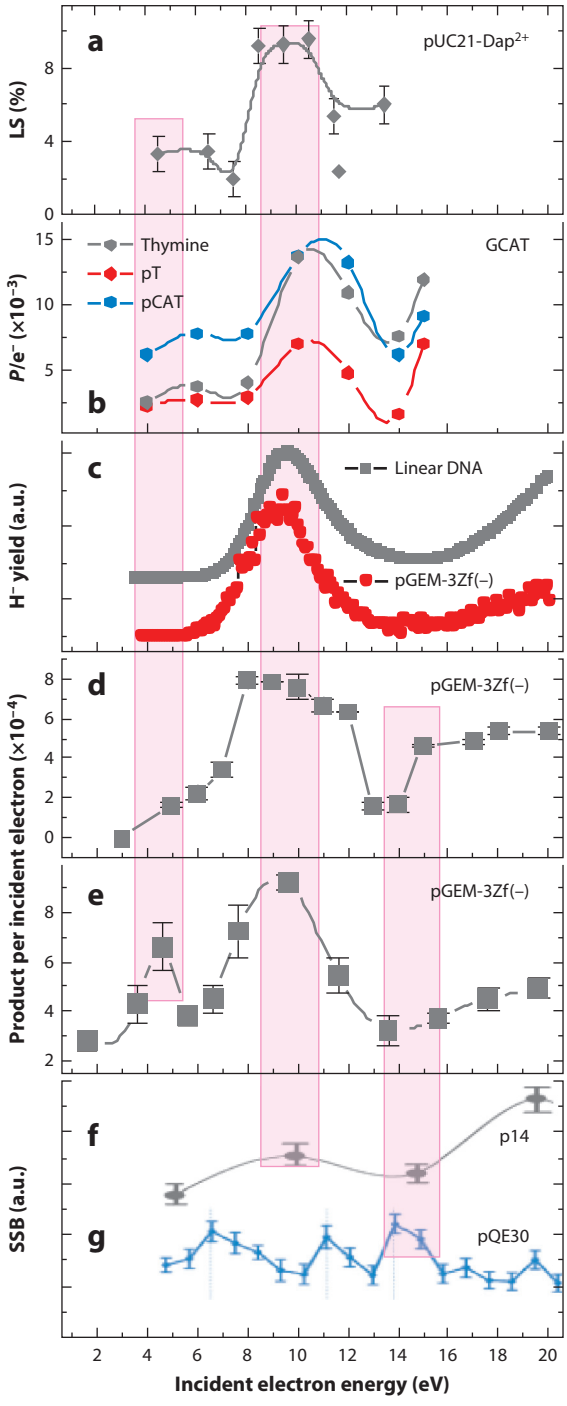

Figure 2

Comparisons of DNA damage induced by 1.6–20-eV electron impact on DNA films comprising (*a*) pUC21 plasmid DNA–diaminopropane cation complexes ($DNA\text{-}Dap^{2+}$) (94), (*b*) the oligonucleotide GCAT integrating the four DNA bases (95), (*c*) 40-bp linear DNA and pGEM-3Zf(−) plasmid DNA (96), (*d*,*e*) pGEM-3Zf(−) plasmid DNA (15, 97), (*f*) p14 plasmid DNA (50), and (*g*) pQE30 plasmid DNA (99). Detected damage events were the loss of the supercoiled configuration (LS) (*a*), fragments with products identified in the key (*b*), H^- yield of electron-stimulated desorption (*c*), and single-strand breaks (SSBs) (*d*–*g*). Panels *d* and *e* adapted with permission from Reference 97. Copyright 2014, AIP Publishing LLC.

structure seen in the yield functions in **Figure 2*a–f*** probably arises from contributions of the many core-excited resonances listed in group II in **Table 1**. Most autoionizing decay channels (i.e., pathway 3 in **Figure 1**) lead to higher-lying $\pi \rightarrow \pi^*$ transitions. From their width in the HREEL spectra, many of these TNI states could be dissociative in the Franck-Condon region, and depending on their lifetimes, pathways 2 and 3 in **Figure 1** may be available simultaneously.

Table 1 lists the energies of the resonance peaks found between 8.5 and 11 eV (group II) in the yield functions of H^-, O^-, CN^-, OH^-, and OCN^- arising from thin films of the bases (100) and the tetramer GCAT (92, 93). In GCAT, the H^- signal is by far the strongest and can be compared to that producing the curve in **Figure 2*c*** with a peak near 10 eV. The latter has been interpreted as arising from DEA to the bases (route 2 in **Figure 1**) with a possible smaller contribution from the sugar ring (96). Experiments on thymine and deuterated and methylated uracil at various positions indicate that even at 8.5 eV, H^- loss is not only bond selective but also site selective (85, 90, 101). According to these experiments, the higher-energy features at approximately 9.3 eV in condensed thymine and GCAT could be primarily caused by the H^- loss from the carbon atoms with a contribution of the H^- loss from CH_3. Similar results were also reported in other studies (63) for DEA to small organic molecules (e.g., acetic acid, propanoic acid, and *n*-propyl amine) that contain the methyl group. Accordingly, the pronounced peaks near 10 eV in **Figure 2*c*** and at 9.2 eV in the H^- yield function from GCAT possibly arise essentially from H^- production at the carbon sites of the bases. As explained above, anion ESD is often inhibited at low energies in the condensed phase owing to the attraction created by the polarization potential induced by the TNI. In gas-phase studies, the 4–6-eV DEA resonance producing H^- below 6 eV results from N–H bond cleavage at the N1 and N3 position of thymine and adenine (101–103). The most intense DEA signal arises from thymine at 6.8 eV, but a strong contribution is also seen in the DEA yields of CN^-, giving a peak at 6 eV. OCN^- and CN^- formation from nucleobases requires complex pathways, possibly involving multibond cleavage driven by the high electron affinity of OCN (3.61 eV) and CN (3.82 eV) (64, 87, 92). The anions mentioned in this paragraph and their corresponding neutral radicals do not directly contribute to strand breaks, but the reactive sites created by DEA to the nucleobases could directly or indirectly be involved in the production of other lesions, such as cross-links.

Another resonance region between 14 and 16 eV can be identified in **Figure 2**. The resonance feature, which is the strongest in the yield function in **Figure 2*g***, was also seen at the same energy in the original yield function of SSBs recorded by Huels et al. (16) and Boudaïffa et al. (15). Although its existence is less certain from the data shown in **Figure 2**, it has recently been observed in the SSB yield function of DNA bound to the chemotherapeutic agent cisplatin (104). As seen in **Table 1**, another group (group III) of core-excited resonances exists in the DNA bases between approximately 12 and 16 eV. This group of resonances, which have only been observed in the DEA decay channel, correlates well with the 14–15-eV structure in the yield functions in **Figure 2*d*,*g***. Depending on the branching ratio between pathways 2 and 3 in **Figure 1**, these resonances could be involved in electron transfer to the phosphate group and induce an SSB.

3. LOW-ENERGY-ELECTRON INTERACTIONS UNDER CELLULAR CONDITIONS: INDIRECT EFFECTS

The gas- and condensed-phase experiments with DNA and its constituents discussed above were performed under ultrahigh vacuum (UHV) conditions to prevent environmental impurities from condensing on the surface and allow one to generate a LEE beam with a well-defined energy. Although such experiments provide information on the direct effects of LEEs, they do not reveal how LEEs can indirectly damage DNA. Only a few advances have been made on the indirect effect

of LEEs owing to the experimental difficulties associated with the production and observation of LEEs in aqueous media.

Ideally, to understand how the fundamental mechanisms in LEE-DNA interactions are modified in living cells, investigators should extend the present experimental studies to the more complex dynamic molecular environment of the cell, ones in which the DNA molecule is embedded into more realistic environments containing essentially water, oxygen, histones, and DNA-binding proteins (105). For instance, Ptasińska & Sanche (106) measured the ESD yields of different anions desorbed by 3–20-eV electron impact on GCAT films under hydrated conditions corresponding to 5.25 water molecules per nucleotide. Their results confirmed that adding water to dry DNA results first in the binding of the molecule to the phosphate group at the position of the negatively charged oxygen (107) and then the formation of a complex comprising the tetramer and a water molecule (DNA-H_2O). Such a complex permits the formation of a new type of dissociative core-excited transient anion located on the phosphate group, which decays by O^- desorption with a resonance peak lying at 11–12 eV and, more specifically, OH^- desorption by rupture of the P–O^- bond. H^- desorbs upon LEE impact by dissociation of a transient anion of the complex, which causes bond cleavage on the H_2O molecule in the DNA-H_2O complex. Additionally, DNA damage via DEA induced by LEEs is increased by a factor of approximately 1.6 when an amount of water corresponding to 60% of the first hydration layer is added to vacuum-dried DNA. Although the magnitude of this enhancement is significant, it is much smaller than the modification in various yields of products caused by the first hydration layer of DNA during the radiochemical events that follow the deposition of the energy of LEEs in irradiated cells. Theoretical and experimental studies were concurrently carried out on the diffraction of 5–30-eV electrons in hydrated B-DNA 5′-CCGGCGCCGG-3′ and A-DNA 5′-CGCGAATTCGCG-3′ sequences by Orlando et al. (98). They postulated that dissociative states of an H_2O-DNA complex may contribute to the damage and modify the SSB and DSB yield functions (98, 108). Additionally, Orlando et al. pointed out that the >5-eV threshold energy for DSBs may be correlated with the presence of these complexes. In this case, an initially core-excited resonance can autoionize, yielding electronically excited water-derived states and a LEE. The electronically excited state dissociates, forming reactive oxygen, OH, or hydrogen, which can lead to sugar-phosphate bond breakage. The slow electron can scatter inelastically within a limited mean free path and excite a shape resonance on a base on the opposite side of the strand. The combination of these two energy loss channels can lead to a DSB. This type of DSB requires the presence of water and is difficult to repair because of the close proximity of damage sites.

Recent work using graphene-coated gold thin films also pointed out the importance of the presence of water, even for DNA damage mediated by shape resonances (38). This likely results from the influence of water on lowering the barrier for charge transfer from the base to the sugar-phosphate bond. In addition, the binding interaction of DNA with graphene allows direct coupling to the phosphates as well as more direct scattering with the guanine and adenine bases. Electrons that have not been captured by DNA bases can be captured by graphene and immediately transferred over 200 nm within <0.36 ps. The environmental or graphene substrate interactions are critical, and at least two mechanisms occur simultaneously during DNA damage on monolayer graphene: direct base capture and ballistic transfer from graphene.

Alizadeh and colleagues (40, 109) have recently developed an alternative approach to simulate cellular conditions to investigate LEE-induced DNA damage under atmospheric conditions and at different levels of humidity and oxygen. Thin films of plasmid DNA deposited on gold and glass substrates were exposed to 1.5-keV Al Kα X-rays. The general features of the SE emission from the metallic surfaces exposed by primary X-ray photons are well understood; in particular, we know that more than 96% of SEs emitted from tantalum lie below 30 eV, with an energy distribution

peaking at approximately 1.4 eV. Whereas the damage yields for DNA deposited on glass result from soft X-rays, those arising from DNA on gold result from the interaction of both X-rays (1.5 keV) and photo-ejected LEEs (an average energy of 5.85 eV) from the metal. The differences in the yields of strand-break damage in samples deposited on the two different substrates can be attributed to the interaction of LEEs with the DNA and its surrounding atmosphere.

Alizadeh & Sanche (110) used this technique to investigate the effect of the presence of some cellular components (e.g., O_2, H_2O, and O_2-H_2O) in the vicinity of DNA molecules. They observed that under an oxygenated environment in humid DNA films, the additional LEE-induced damage resulting from the combination of water and oxygen exhibits a superadditive effect, which leads to the formation of DSBs with a yield almost seven times higher than that obtained by X-ray photons. More recently, Alizadeh and colleagues (111) reported the formation of four radiation-induced products from thymidine by soft X-rays and LEEs [i.e., base release, and base modification including 5-hydroxymethyl-2′-deoxyuridine (5-HMdUrd), 5-formyl-2′-deoxyuridine (5-FordUrd), and 5,6-dihydrothymidine (5,6-DHT)]. Among the products analyzed, thymine release is the predominant channel, which arises from *N*-glycosidic-bond cleavage involving the π^* low-lying TNI. A LEE-mediated mechanism was proposed to explain the observation of the nucleobase modifications 5-HMdUrd and 5-FordUrd, which involve loss of hydride (H^-) from the methyl group site via DEA. *G* values derived from these experiments show that the formation of free thymine, 5-HMdUrd, and 5-FordUrd is favored within an O_2 atmosphere compared to a nitrogenous environment, as more radicals and ions are formed owing to the interaction of radiation with O_2, which are in turn considerably more reactive than those generated in an N_2 environment. Additionally, O_2 can react with carbon-centered radicals, thereby fixing the damage. In contrast, no 5,6-DHT was detected when samples were irradiated under an O_2 atmosphere, indicating that O_2 molecules react with the intermediate radical compound inhibiting the pathway to the formation of 5,6-DHT (111).

The decay mechanisms of electronic excitations and correlated electron interactions are the subject of intense study. Cederbaum and colleagues (112–114) proposed a novel electronic decay mechanism of inner valence levels, which should be common in weakly interacting complexes. In the case of complexes involving molecules, this process is referred to as intermolecular Coulomb decay (ICD) and is possible mainly because of the couplings and interactions induced by the local environment. Briefly, ICD follows from the production of an inner valence hole that is filled by an outer valence electron on the same center, followed by energy exchange with a neighbor in the complex and the ejection of an outer valence electron from this neighboring site. SE emission from the neighboring site can occur as a result of energy transfer. The energy of the ICD electron is low and typically below 10 eV. ICD is expected to take place universally in weakly bound aggregates containing light atoms and may be an unappreciated source of LEEs. Although most researchers have concentrated on gas-phase targets in their ICD measurements, recent studies have observed ICD in large water clusters (115) or at condensed-phase interfaces containing water clusters (116).

Significant uncontrolled damage to molecules such as DNA is associated with the onset of cancer, whereas controlled interactions and the local release of LEEs can be used as effective therapeutic cancer treatment agents. As the ejection of slow electrons is a clear result of ICD, it has been proposed that ICD can play a role in the formation of both SSBs and DSBs in DNA (112, 116, 117). Grieves & Orlando (116) estimated that ICD may contribute up to 50% of the SSB probability for >20-eV ionization events directly at the DNA-water interface. Because the formation of DSBs requires excitation energies >5 eV, the impact on DSBs is expected to be much lower.

If ICD contributes significantly to DNA damage, this could be exploited during X-ray treatment of cancer. Indeed, as shown in **Figure 3**, the exploitation of X-ray interactions with gold

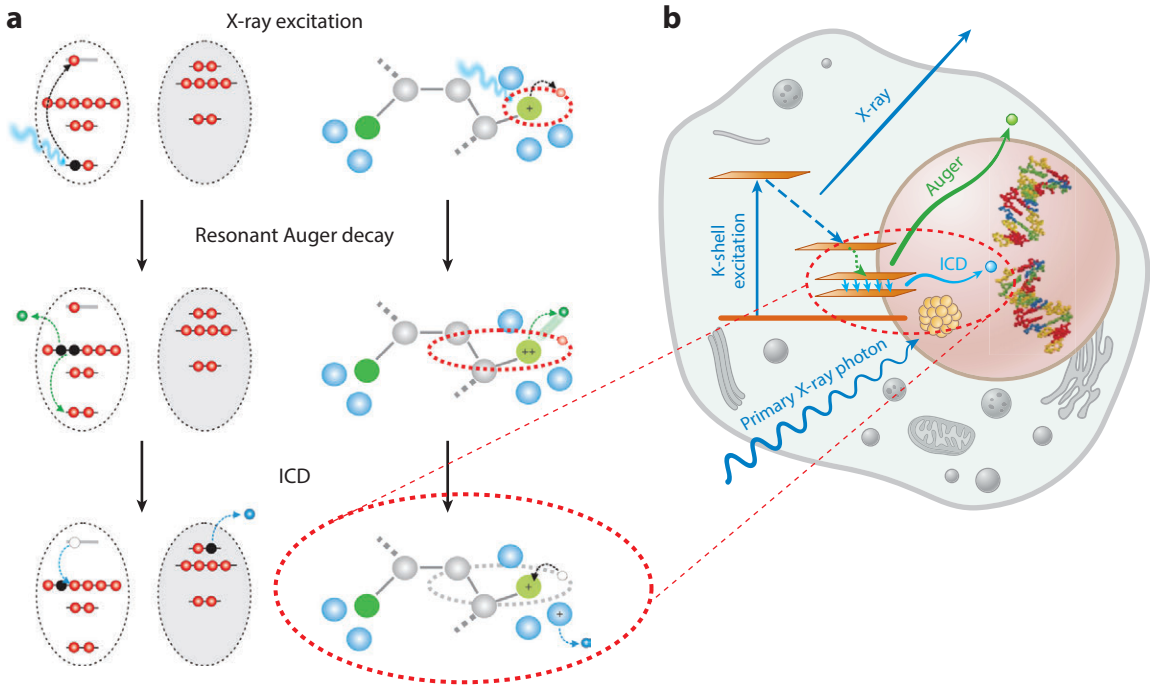

Figure 3

(*a*) Resonant Auger decay process following X-ray excitation. A second process known as interatomic or intermolecular Coulomb decay (ICD) can also occur, leading to the ejection of slow electrons and adjacent holes. (*b*) Possible exploitation of gold nanoparticles and ICD in the controlled radiation damage of cells. Figure adapted from Reference 112 with permission from Macmillan Publishers Ltd, copyright 2014.

nanoparticles within cells and the subsequent release of both Auger and ICD electrons have been suggested as possible targeted cancer treatment strategies (112).

4. CELL DEATH INDUCED BY LOW-ENERGY ELECTRONS

Although LEEs are well known to induce SSBs and DSBs in DNA, it is only very recently that their cellular lethality has been demonstrated by Kouass Sahbani et al. (118), who investigated the biological functionality of DNA, via a simple model system comprising *Escherichia coli* transformed with a LEE-irradiated plasmid [pGEM-3Zf(−)] DNA (119). In these experiments, highly ordered DNA films were prepared on pyrolitic graphite by molecular self-assembly using Dap ions to bind together the plasmids (119) and were bombarded in UHV with 10-eV electrons (118). The assembly mimics the amino groups of the lysine and arginine amino acids within the histone proteins. Cell survival was measured as a function of LEE-induced damage to supercoiled DNA, which possessed an ampicillin resistance gene. A portion of the sample was analyzed for SSBs, DSBs, and duplex cross-links (119). Cluster lesions, which included base damage, were analyzed by treating the irradiated samples with *E. coli* base excision repair endonuclease III (Nth) or formamidopyrimidine-DNA *N*-glycosylase (Fpg) (9). The other portion of the sample was introduced into *E. coli* JM109 bacteria, which are devoid of any genes coding for resistance to the antibiotic ampicillin and thus rely on the integrity of the pGEM-3Zf(−) plasmid for survival. The bacteria were incubated with ampicillin, and the number of colonies was counted. From

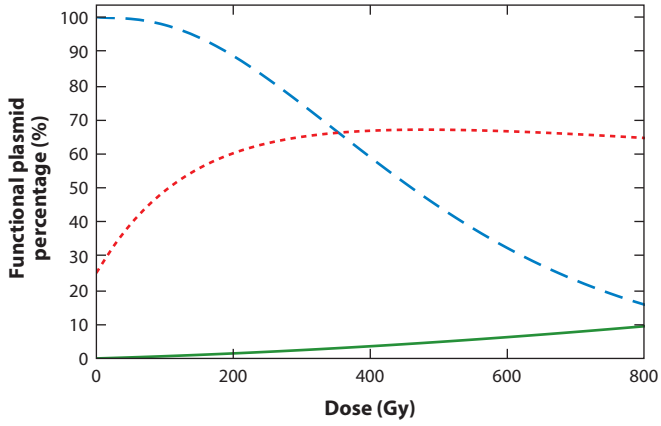

Figure 4

Biological activity of the plasmid pGEM-3Zf(−) following 10-eV electron irradiation. The dashed curve represents the survival function of the plasmid, and the dotted line is the variation in the entry function; both are plotted as a function of electron fluence. The behavior of the entry function results from the change in the number of plasmids with different entry coefficients. The solid line shows the formation of linear plasmids as a function of electron fluence.

dose-response curves, yields of surviving bacteria per LEE per DNA bombarded were obtained. Because *E. coli* cannot survive without a functional plasmid in the presence of ampicillin, these yields were proportional to the number of initially undamaged plasmids, the ability of different DNA configurations to enter the cell, the type of damage, and the capacity of the cell to repair that damage.

Figure 4 shows the two components of the transformation efficiency: the entry efficiency and the functionality of the plasmid transformed into wild-type *E. coli* (JM109) as a function of electron fluence. The survival curve in **Figure 4** (i.e., the plasmid functionality) has a definite plateau at low electron fluence followed by an exponential loss of viability. This behavior suggests that the lethal lesions can be repaired when present at low levels, but at higher levels, the repair process is overwhelmed and results in plasmid inactivation. DSBs are known to be toxic, but the yields induced by LEE impact [(3.9 ± 0.6) DSB $\times 10^{-16}$ cm^2 per plasmid] were far too low to explain the loss of plasmid functionality. The yield for total non-DSB cluster damage was approximately 2.6 times higher than that of DSBs [(3.9 ± 0.6) DSB $\times 10^{-16}$ cm^2 per plasmid versus (1.5 ± 0.2) DSB $\times 10^{-16}$ cm^2 per plasmid] but was still too low to explain the toxicity of LEE irradiation. However, the yields of unknown lethal damage, which could be DNA-diamine cross-links, analogous to DNA-histone cross-links, were 28 times higher than the yields of non-DSB cluster damage. Thus, the results of Kouass Sahbani et al. (118) indicate that the majority of the lethal lesions induced by LEEs are neither DSB nor non-DSB cluster lesions and that LEEs could be efficient at causing intermolecular cross-links to form adducts, which are refractory to repair and result in the loss of DNA functionality.

5. SUMMARY AND CONCLUSIONS

In an effort to explain how LEEs damage the human genome, investigators have focused on understanding LEE interactions with bacterial plasmids, DNA bases, sugar analogs, phosphate groups, longer DNA moieties, and DNA under conditions that mimic the cellular environment.

Results obtained by several laboratories on biomolecular films prepared and analyzed by different methods and irradiated with different electron-beam current densities and fluencies show a striking resemblance in the amount and type of damage produced. Specifically, it has been shown that two major types of TNIs are involved in LEE-induced damage to DNA: shape resonances, which consist of an electron temporarily occupying a previous unfilled orbital of the ground state of a basic subunit, and core-excited or Feshbach resonances, in which the incoming electron is captured by the positive electron affinity of an electronically excited state of the subunit. A TNI can decay by DEA usually with the concomitant formation of a stable anion and a radical. These fragments can be released from DNA, but in large biomolecules, chain cleavage, leaving one side with the electron and the other as a radical, is also an important process. Alternatively, autoionization of a core-excited anion site can cause bond rupture by leaving the subunit in a dissociative electronically excited state. This process can create a DSB in dry or hydrated DNA, when the detaching electron transfers to the opposite strand (97, 98). In the case of a water-DNA interface, TNI states of H_2O-DNA complexes can decay via autoionization, releasing a LEE (<1 eV) and an electronically excited site in the vicinity of a base or sugar. The slow electron can form a shape resonance, leading to a strand break, whereas the electronically excited target can dissociate into reactive radicals, such as O or OH. These can also form with background O_2 and react with the nearby sugar-phosphate bond, giving rising to a DSB that is in close proximity. These DSBs occurring above 5 eV, which are correlated with the presence of water, are difficult to repair, and are thus likely to be associated with the appearance of cancer cells initiated by ionizing radiation. Controlling DNA damage using molecular and nanoparticle targets with high LEE yields may be useful in targeted radiation-based cancer therapies.

DISCLOSURE STATEMENT

The authors are not aware of any affiliations, memberships, funding, or financial holdings that might be perceived as affecting the objectivity of this review.

ACKNOWLEDGMENTS

Financial support for this work was provided by the Canadian Institutes of Health Research (MOP81356). T.M.O. thanks the US Department of Energy, Office of Science (contract DOE-FG02-02ER15337) for support.

LITERATURE CITED

1. Hall EJ, Giaccia AJ, eds. 2006. *Radiobiology for the Radiologist*. Philadelphia: Lippincott Williams & Wilkins. 6th ed.
2. O'Driscoll M, Jeggo PA. 2006. The role of double-strand break repair: insights from human genetics. *Nat. Rev. Genet.* 7:45–54
3. Lehnert S. 2008. *Biomolecular Action of Ionizing Radiation*. London: Taylor & Francis
4. von Sonntag C. 1987. *The Chemical Basis of Radiation Biology*. London: Taylor & Francis
5. Sevilla MD, Bernhard WA. 2008. Mechanisms of direct radiation damage to DNA. In *Radiation Chemistry: From Basics to Applications in Material and Life Sciences*, ed. M Spotheim-Maurizot, M Mostafavi, T Douki, J Belloni, pp. 191–201. Les Ulis, Fr.: EDP Sci.
6. Uehara S, Nikjoo H, Goodhead DT. 1999. Comparison and assessment of electron cross sections for Monte Carlo track structure codes. *Radiat. Res.* 152:202–13
7. Wishart JF, Rao BMS. 2010. *Recent Trends in Radiation Chemistry*. Singapore: World Sci.
8. O'Neill P. 2001. Radiation-induced damage in DNA. In *Radiation Chemistry: Present Status and Future Trends*, pp. 585–622. Amsterdam: Elsevier Sci.

9. Michael BD, O'Neill PA. 2000. A sting in the tail of electron tracks. *Science* 287:1603–4
10. Nguyen J, Ma Y, Luo T, Bristow RG, Jaffray DA, Lu QB. 2011. Direct observation of ultrafast-electron-transfer reactions unravels high effectiveness of reductive DNA damage. *Proc. Natl. Acad. Sci. USA* 108:11778–83
11. Bald I, Illenberger E, Kopyra I. 2012. Damage of DNA by low energy electrons (<3 eV). *J. Phys. Conf. Ser.* 373:012008
12. Märk TD, Hatano Y, Linder F. 1995. Electron collision cross sections. In *Atomic and Molecular Data for Radiotherapy and Radiation Research*, pp. 163–275. IAEA-TECDOC-799. Vienna: Int. At. Energy Agency
13. von Sonntag C. 2006. *Free-Radical-Induced DNA Damage and Its Repair: A Chemical Perspective*. Berlin: Springer-Verlag
14. Pimblott SM, LaVerne JA. 2007. Production of low-energy electrons by ionizing radiation. *Phys. Chem.* 76:1244–47
15. Boudaïffa B, Cloutier P, Hunting DJ, Huels MA, Sanche L. 2000. Resonant formation of DNA strand breaks by low-energy (3 to 20 eV) electrons. *Science* 287:1658–60
16. Huels MA, Boudaïffa B, Cloutier P, Hunting DJ, Sanche L. 2003. Single, double, and multiple double strand breaks induced in DNA by 3–100 eV electrons. *J. Am. Chem. Soc.* 125:4467–77
17. Alizadeh E, Sanz AG, Garcia G, Sanche L. 2013. Radiation damage to DNA: the indirect effect of low-energy electrons. *J. Phys. Chem. Lett.* 4:820–25
18. Rezaee M, Alizadeh A, Hunting DJ, Sanche L. 2014. A single ultra-low energy electron (0.5 eV) can induce a double strand break in DNA modified by platinum chemotherapeutic drugs. *Chem. Med. Chem.* 9:1145–49
19. Kopyra J, Keller A, Bald I. 2014. On the role of fluoro-substituted nucleosides in DNA radiosensitization for tumor radiation therapy. *RSC Adv.* 4:6825–29
20. Zheng Y, Cloutier P, Hunting DJ, Sanche L. 2008. Radiosensitization by gold nanoparticles: comparison of DNA damage induced by low and high-energy electrons. *J. Biomed. Nanotechnol.* 4:469–73
21. Sanche L. 2009. Role of secondary low energy electrons in radiobiology and chemoradiation therapy of cancer. *Chem. Phys. Lett.* 474:1–6
22. Zheng Y, Hunting DJ, Ayotte P, Sanche L. 2008. Role of secondary low-energy electrons in the concomitant chemoradiation therapy of cancer. *Phys. Rev. Lett.* 100:198101
23. Rezaee M, Hunting DJ, Sanche L. 2013. New insights into the mechanism underlying the synergistic action of ionizing radiation with platinum chemotherapeutic drugs: the role of low-energy electrons. *Int. J. Radiat. Oncol. Biol. Phys.* 87:847–53
24. Rezaee M, Sanche L, Hunting DJ. 2013. Cisplatin enhances the formation of DNA single- and double-strand breaks by hydrated electrons and hydroxyl radicals. *Radiat. Res.* 179:323–31
25. Tippayamontri T, Kobt R, Paquette B, Sanche L. 2011. Cellular uptake and cytoplasm/DNA distribution of cisplatin and oxaliplatin and their liposomal formulation in human colorectal cancer cell HCT116. *Investig. New Drugs* 29:1321–27
26. Alizadeh E, Sanche L. 2012. Precursors of solvated electrons in radiobiological physics and chemistry. *Chem. Rev.* 112:5578–602
27. Baccarelli I, Bald I, Gianturco FA, Illenberger E, Kopyra J. 2011. Electron-induced damage of DNA and its components: experiments and theoretical models. *Phys. Rep.* 508:1–44
28. Sanche L. 2009. Low-energy electron interaction with DNA: bond dissociation and formation of transient anions, radicals, and radical anions. In *Radical and Radical Ion Reactivity in Nucleic Acid Chemistry*, ed. MM Greenberg, pp. 239–95. New York: Wiley
29. Sanche L. 2005. Low energy electron-driven damage in biomolecules. *Eur. Phys. J. D* 35:367–90
30. Gu J, Leszczynski J, Schaefer HF. 2012. Interactions of electrons with bare and hydrated biomolecules: from nucleic acid bases to DNA segments. *Chem. Rev.* 112:5603–40
31. Arumainayagam CR, Lee H, Nelson RB, Haines DR, Gunawardane R. 2010. Low-energy electron-induced reactions in condensed matter. *Surf. Sci. Rep.* 65:1–44
32. Zheng Y, Sanche L. 2013. Low energy electrons in nanoscale radiation physics: relationship to radiosensitization and chemoradiation therapy. *Rev. Nanosci. Nanotechnol.* 2:1–28
33. Allan M. 2007. Absolute angle-differential elastic and vibrational excitation cross sections for electron collisions with tetrahydrofuran. *J. Phys. B* 40:3531–44

34. Lévesque PL, Michaud M, Cho W, Sanche L. 2005. Absolute electronic excitation cross sections for low-energy electron (5–12 eV) scattering from condensed thymine. *J. Chem. Phys.* 122:224704
35. Bazin M, Michaud M, Sanche L. 2010. Absolute cross sections for electronic excitations of cytosine by low energy electron impact. *J. Chem. Phys.* 133:155104
36. Panajotović R, Michaud M, Sanche LL. 2007. Cross sections for low-energy electron scattering from adenine in the condensed phase. *Phys. Chem. Chem. Phys.* 9:138–48
37. Keller A, Bald I, Rotaru A, Cauët E, Gothelf KV, Besenbacher F. 2012. Probing electron-induced bond cleavage at the single-molecule level using DNA origami templates. *ACS Nano* 6:4392–99
38. Sidorov AN, Orlando TM. 2013. Monolayer graphene platform for the study of DNA damage by low-energy electron irradiation. *J. Phys. Chem. Lett.* 4:2328–33
39. Han X, Klas M, Liu Y, Stack MS, Ptasińska S. 2013. DNA damage in oral cancer cells induced by nitrogen atmospheric pressure plasma jets. *Appl. Phys. Lett.* 102:233703
40. Alizadeh E, Sanche L. 2014. Low-energy-electron interactions with DNA: approaching cellular conditions with atmospheric experiments. *Eur. Phys. J. D* 68:97–110
41. Rosenberg RA, Symonds JM, Vijayalakshima K, Mishra D, Orlando TM, Naaman R. 2014. The relationship between interfacial bonding and radiation damage in adsorbed DNA. *Phys. Chem. Chem. Phys.* 16:15319–25
42. Bald I, Langer J, Tegeder P, Ingólfsson O. 2008. From isolated molecules through clusters and condensates to the building blocks of life. *Int. J. Mass Spectrom.* 277:4–25
43. Allan M. 1989. Study of triplet states and short-lived negative ions by means of electron impact spectroscopy. *J. Electron. Spectrosc. Relat. Phenom.* 48:219–351
44. Caron L, Sanche L. 2012. Theoretical studies of electron interactions with DNA and its subunits. In *Low-Energy Electron Scattering from Molecules, Biomolecules and Surfaces*, ed. P Čársky, R Čurik, pp. 161–230. Boca Raton, FL: CRC
45. Lepage M, Letarte S, Michaud M, Motte-Tollet F, Hubin-Franskin MJ, et al. 1998. Electron spectroscopy of resonance-enhanced vibrational excitations of gaseous and solid tetrahydrofuran. *J. Chem. Phys.* 109:5980–86
46. Colyer CJ, Vizcaino V, Sullivan JP, Brunger MJ, Buckman SJ. 2007. Absolute elastic cross-sections for low-energy electron scattering from tetrahydrofuran. *New J. Phys.* 9:41
47. Możejko P, Ptasińska-Denga E, Domaracka A, Szmytkowski C. 2006. Absolute total cross-section measurements for electron collisions with tetrahydrofuran. *Phys. Rev. A* 74:012708
48. Milosavljević AR, Šević D, Marinković BP. 2008. Electron interaction with deoxyribose analogue molecules in gaseous phase. *J. Phys. Conf. Ser.* 101:012014
49. Abdoul-Carime H, Cloutier P, Sanche L. 2001. Low-energy (5–40 eV) electron-stimulated desorption of anions from physisorbed DNA bases. *Radiat. Res.* 155:625–33
50. Chen Y, Aleksandrov A, Orlando TM. 2008. Probing low-energy electron induced DNA damage using single photon ionization mass spectrometry. *Int. J. Mass Spectrom.* 277:314–20
51. Schulz GJ. 1973. Resonances in electron impact on diatomic molecules. *Rev. Mod. Phys.* 45:423–86
52. Christophorou LG, Olthoff JK. 2004. *Fundamental Electron Interactions with Plasma Processing Gases*. Dordrecht: Kluwer Acad.
53. Read FJ. 1977. A modified Rydberg formula. *J. Phys. B* 10:449–58
54. Mott NF, Massey HSW. 1965. *The Theory of Atomic Collisions*. Oxford: Clarendon. 3rd ed.
55. Skalick T, Allan M. 2004. The assignment of dissociative electron attachment bands in compounds containing hydroxyl and amino groups. *J. Phys. B* 37:4849–59
56. Ibănescu BC, Allan M. 2009. Selective cleavage of the C–O bonds in alcohols and asymmetric ethers by dissociative electron attachment. *Phys. Chem. Chem. Phys.* 11:7640–48
57. Ibănescu BC, May O, Monney A, Allan M. 2007. Electron-induced chemistry of alcohols. *Phys. Chem. Chem. Phys.* 9:3163–73
58. Ibănescu BC, May O, Allan M. 2008. Differences in the cleavage of the ether bond by electron impact in linear ethers and in tetrahydrofuran. *Phys. Chem. Chem. Phys.* 10:1507–11
59. Ibănescu BC, Allan M. 2008. A dramatic difference between the electron-driven dissociation of alcohols and ethers and its relation to Rydberg states. *Phys. Chem. Chem. Phys.* 10:5232–37

60. Jungen M, Vogt J, Staemmler V. 1979. Feshbach resonances and dissociative electron attachment of H_2O. *Chem. Phys.* 37:49–55
61. Kühn A, Fenzlaff HP, Illenberger E. 1988. Formation and dissociation of negative ion resonances in methanol and allylalcohol. *J. Chem. Phys.* 88:7453–58
62. Curtis MG, Walker IC. 1992. Dissociative electron attachment in water and methanol (5–14 eV). *J. Chem. Soc. Faraday Trans.* 88:2805–10
63. Prabhudesai VS, Kelkar AH, Nandi D, Krishnakumar E. 2005. Functional group dependent site specific fragmentation of molecules by low energy electrons. *Phys. Rev. Lett.* 95:143202
64. Prabhudesai VS, Nandi D, Kelkar AH, Krishnakumar E. 2008. Functional group dependent dissociative electron attachment to simple organic molecules. *J. Chem. Phys.* 128:154309
65. Prabhudesai VS, Ram NB, Aravind G, Rawat P, Krishnakumar E. 2007. Probing site selective fragmentation of molecules containing hydroxyl group using Velocity Slice Imaging. *J. Phys. Conf. Ser.* 80:012016
66. Orzol M, Martin I, Kocisek J, Dabkowska I, Langer J, Illenberger E. 2007. Bond and site selectivity in dissociative electron attachment to gas phase and condensed phase ethanol and trifluoroethanol. *Phys. Chem. Chem. Phys.* 9:3424–31
67. Kumar A, Sevilla MD. 2009. Theoretical modeling of radiation-induced DNA damage. In *Radical and Radical Ion Reactivity in Nucleic Acid Chemistry*, ed. MM Greenberg, pp. 1–40. New York: Wiley
68. Kumar A, Sevilla MD. 2008. The role of $\pi\sigma^*$ excited states in electron-induced DNA strand break formation: a time-dependent density functional theory study. *J. Am. Chem. Soc.* 130:2130–31
69. Martin F, Burrow PD, Cai Z, Cloutier P, Hunting DJ, Sanche L. 2004. DNA strand breaks induced by 0–4 eV electrons: the role of shape resonances. *Phys. Rev. Lett.* 93:068101
70. Li X, Sevilla MD, Sanche L. 2003. Density functional theory studies of electron interaction with DNA: Can zero eV electrons induce strand breaks? *J. Am. Chem. Soc.* 125:13668–69
71. Zheng Y, Cloutier P, Hunting DJ, Sanche L, Wagner JR. 2005. Chemical basis of DNA sugar-phosphate cleavage by low-energy electrons. *J. Am. Chem. Soc.* 127:16592–98
72. Barrios R, Skurski P, Simons J. 2002. Mechanism for damage to DNA by low-energy electrons. *J. Phys. Chem. B* 106:7991–94
73. Berdys J, Anusiewicz I, Skurski P, Simons J. 2004. Damage to model DNA fragments from very low-energy (<1 eV) electrons. *J. Am. Chem. Soc.* 126:6441–47
74. Berdys J, Skurski P, Simons J. 2004. Damage to model DNA fragments by 0.25–1.0 eV electrons attached to a thymine π^* orbital. *J. Phys. Chem. B* 108:5800–5
75. Berdys J, Anusiewicz I, Skurski P, Simons J. 2004. Theoretical study of damage to DNA by 0.2–1.5 eV electrons attached to cytosine. *J. Phys. Chem. A* 108:2999–3005
76. Smyth M, Kohanoff J. 2011. Excess electron localization in solvated DNA bases. *Phys. Rev. Lett.* 106:238108
77. Dabkowska I, Rak J, Gutowski M. 2005. DNA strand breaks induced by concerted interaction of H radicals and low-energy electrons. *Eur. Phys. J. D* 35:429–35
78. Zheng Y, Wagner JR, Sanche L. 2006. DNA damage induced by low-energy electrons: electron transfer and diffraction. *Phys. Rev. Lett.* 96:208101
79. Caron LG, Sanche L. 2005. Diffraction in resonant electron scattering from helical macromolecules: effects of the DNA backbone. *Phys. Rev. A* 72:032726
80. Caron LG, Sanche L. 2003. Low-energy electron diffraction and resonances in DNA and other helical macromolecules. *Phys. Rev. Lett.* 91:113201
81. Li Z, Zheng Y, Cloutier P, Sanche L, Wagner JR. 2008. Low energy electron induced DNA damage: effects of terminal phosphate and base moieties on the distribution of damage. *J. Am. Chem. Soc.* 130:5612–13
82. Park Y, Li Z, Cloutier P, Sanche L, Wagner JR. 2010. DNA damage induced by low-energy electrons: conversion of thymine to 5,6-dihydrothymine in the oligonucleotide trimer TpTpT. *Radiat. Res.* 175:240–46
83. Li Z, Cloutier P, Sanche L, Wagner JR. 2011. Low-energy electron-induced damage in a trinucleotide containing 5-bromouracil. *J. Phys. Chem. B* 115:13668–73

84. Ptasińska S, Denifl S, Grill V, Märk TD, Scheier P, et al. 2005. Bond-selective H-ion abstraction from thymine. *Angew. Chem. Int. Ed. Engl.* 44:1647–50
85. Abdoul-Carime H, Langer J, Huels MA, Illenberger E. 2005. Decomposition of purine nucleobases by very low energy electrons. *Eur. Phys. J. D* 35:399–404
86. Denifl S, Ptasińska S, Cingel M, Matejcik S, Scheier P, Märk TD. 2003. Electron attachment to the DNA bases thymine and cytosine. *Chem. Phys. Lett.* 377:74–80
87. Denifl S, Ptasińska S, Probst M, Hrušák J, Scheier P, Märk TD. 2004. Electron attachment to the gas-phase DNA bases cytosine and thymine. *J. Phys. Chem. A* 108:6562–69
88. Denifl S, Zappa F, Mähr I, Lecointre J, Probst M, et al. 2006. Mass spectrometric investigation of anions formed upon free electron attachment to nucleobase molecules and clusters embedded in superfluid helium droplets. *Phys. Rev. Lett.* 97:043201
89. Huber D, Beikircher M, Denifl S, Zappa F, Matejcik S, et al. 2006. High resolution dissociative electron attachment to gas phase adenine. *J. Chem. Phys.* 125:084304
90. Ptasińska S, Denifl S, Grill V, Märk TD, Illenberger E, Scheier P. 2005. Bond- and site-selective loss of H^- from pyrimidine bases. *Phys. Rev. Lett.* 95:093201
91. Ptasińska S, Denifl S, Mróz B, Probst M, Grill V, et al. 2005. Bond selective dissociative electron attachment to thymine. *J. Chem. Phys.* 123:124302
92. Ptasińska S, Sanche L. 2006. On the mechanism of anion desorption from DNA induced by low energy electrons. *J. Chem. Phys.* 125:144713
93. Ptasińska S, Sanche L. 2007. Dissociative electron attachment to abasic DNA. *Phys. Chem. Chem. Phys.* 9:1730–35
94. Boulanouar O, Fromm M, Bass AD, Cloutier P, Sanche L. 2013. Dissociative electron attachment to DNA-diamine thin films: impact of the DNA close environment on the OH^- and O^- decay channels. *J. Chem. Phys.* 139:055104
95. Zheng Y, Cloutier P, Hunting DJ, Wagner JR, Sanche L. 2006. Phosphodiester and *N*-glycosidic bond cleavage in DNA induced by 4–15 eV electrons. *J. Chem. Phys.* 124:064710
96. Pan X, Cloutier P, Hunting DJ, Sanche L. 2003. Dissociative electron attachment to DNA. *Phys. Rev. Lett.* 90:208102
97. Luo X, Zheng Y, Sanche L. 2014. DNA strand breaks and crosslinks induced by transient anions in the range 2–20 eV. *J. Chem. Phys.* 140:155101
98. Orlando TM, Oh D, Chen Y, Aleksandrov A. 2008. Low-energy electron diffraction and induced damage in hydrated DNA. *J. Chem. Phys.* 128:195102
99. Kumar S, Pota T, Peri D, Dongre A, Rao B. 2012. Low energy electron induced damage to plasmid DNA pQE30. *J. Chem. Phys.* 137:045101
100. Abdoul-Carime H, Cloutier P, Sanche L. 2001. Low-energy (5–40 eV) electron-stimulated desorption of anions from physisorbed DNA bases. *Radiat. Res.* 155:625–33
101. Ptasińska S, Denifl S, Scheier P, Illenberger E, Märk TD. 2005. Bond- and site-selective loss of H atoms from nucleobases by very-low-energy electrons (<3 eV). *Angew. Chem. Int. Ed. Engl.* 44:6941–43
102. Ptasińska S, Denifl S, Gohlke S, Scheier P, Illenberger E, Märk TD. 2006. Decomposition of thymidine by low-energy electrons: implications for the molecular mechanisms of single-strand breaks in DNA. *Angew. Chem. Int. Ed. Engl.* 45:1893–96
103. Burrow PD, Gallup GA, Scheer AM, Denifl S, Ptasińska S, et al. 2006. Vibrational Feshbach resonances in uracil and thymine. *J. Chem. Phys.* 124:124310
104. Bao Q, Chen Y, Zheng Y, Sanche L. 2014. Cisplatin radiosensitization of DNA irradiated with 2–20 eV electrons: role of transient anions. *J. Phys. Chem. C* 118:15516–24
105. Solomun T, Skalicky T. 2008. The interaction of a protein–DNA surface complex with low-energy electrons. *Chem. Phys. Lett.* 453:101–4
106. Ptasińska S, Sanche L. 2007. Dissociative electron attachment to hydrated single DNA strands. *Phys. Rev. E* 75:031915
107. Falk M, Hartman KA, Lord RC. 1963. Hydration of deoxyribonucleic acid. II. An infrared study. *J. Am. Chem. Soc.* 85:387–91

108. Grieves GA, McLain JL, Orlando TM. 2011. Low-energy electron-stimulated reactions in nanoscale water films and water-DNA interfaces. In *Charged Particle and Photon Interactions with Matter: Recent Advances, Applications, and Interfaces*, ed. Y Hatano, Y Katsumura, A Mozumder, pp. 473–501. Boca Raton, FL: CRC
109. Alizadeh E, Cloutier P, Hunting DJ, Sanche L. 2011. Soft X-ray and low energy electron-induced damage to DNA under N_2 and O_2 atmospheres. *J. Phys. Chem. B* 115:4523–31
110. Alizadeh E, Sanche L. 2013. The role of humidity and oxygen level on damage to DNA induced by soft X-rays and low-energy electrons. *J. Phys. Chem. C* 117:22445–53
111. Alizadeh E, Sanz AG, Madugundu GS, Garcia G, Wagner JR, Sanche L. 2014. Thymidine decomposition induced by low-energy electrons and soft X-rays under N_2 and O_2 atmospheres. *Radiat. Res.* 181:629–40
112. Gokhberg K, Kolorenč P, Kuleff AI, Cederbaum LS. 2014. Site- and energy-selective slow-electron production through intermolecular Coulombic decay. *Nature* 505:661–63
113. Cederbaum LS, Zobeley J, Tarantelli F. 1997. Giant intermolecular decay and fragmentation of clusters. *Phys. Rev. Lett.* 79:4778–81
114. Santra R, Zobeley J, Cederbaum LS, Moiseyev N. 2000. Interatomic coulombic decay in van der Waals clusters and impact of nuclear motion. *Phys. Rev. Lett.* 85:4490–93
115. Mucke M, Braune M, Barth S, Förstel M, Lischke T, et al. 2010. A hitherto unrecognized source of low-energy electrons in water. *Nat. Phys.* 6:143–46
116. Grieves GA, Orlando TM. 2011. Intermolecular coulomb decay at weakly coupled heterogeneous interfaces. *Phys. Rev. Lett.* 107:016104
117. Hergenhan U. 2012. Production of low kinetic energy electrons and energetic ion pairs by Intermolecular Coulombic Decay. *Int. J. Radiat. Biol.* 88:871–83
118. Kouass Sahbani S, Sanche L, Cloutier P, Bass AD, Hunting DJ. 2014. Loss of cellular transformation efficiency induced by DNA irradiation with low-energy (10 eV) electrons. *J. Phys. Chem. B* 118:13123–31
119. Kouass Sahbani S, Girouard S, Cloutier P, Sanche L, Hunting DJ. 2014. The relative contributions of DNA strand breaks, base damage and clustered lesions to the loss of DNA functionality induced by ionizing radiation. *Radiat. Res.* 181:99–110